Cox-Voinov theory with slip

Tak S. Chan [1], Catherine Kamal[2], Jacco H. Snoeijer[3], James E. Sprittles[4], and Jens Eggers[5]

[1]Mechanics Division, Department of Mathematics, University of Oslo, Oslo 0316, Norway
[2]School of Engineering and Material Science, Queen Mary University of London, London E1 4NS, United Kingdom
[3]Physics of Fluids Group, Faculty of Science and Technology, Mesa+ Institute, University of Twente, 7500 AE Enschede, the Netherlands
[4]Mathematics Institute, University of Warwick, Coventry CV4 7AL, United Kingdom
[5]School of Mathematics, University of Bristol, University Walk, Bristol BS8 1TW, United Kingdom

(Received xx; revised xx; accepted xx)

Most of our understanding of moving contact lines relies on the limit of small capillary numbers. This means the contact line speed is small compared to the capillary speed γ/η, where γ is the surface tension and η the viscosity, so that the interface is only weakly curved. The majority of recent analytical work has assumed in addition that the angle between the free surface and the substrate is also small, so that lubrication theory can be used. Here, we calculate the shape of the interface near a slip surface for arbitrary angles, and for two phases of arbitrary viscosities, thereby removing a key restriction in being able to apply small capillary number theory.

1. Introduction

The theory of the moving contact line at small capillary numbers was founded by Voinov (1976) and generalized to arbitrary viscosity ratios M by Cox (1986). The problem is that if the no-slip boundary condition were to apply down to arbitrarily small scales (Huh & Scriven 1971; Bonn *et al.* 2009; Snoeijer & Andreotti 2013), a contact line would not be able to move. Therefore, one needs to invoke a small length scale on which the conventional equations for fluid motion are relaxed. The simplest, and often physically realistic, such choice is the introduction of a Navier slip length λ (Lauga *et al.* 2008), over which a fluid may slip past a solid interface. It is generally of the order of a few nanometers, but increases somewhat for hydrophobic surfaces (Barrat & Bocquet 1999; Cottin-Bizonne *et al.* 2005). A slip length is used very widely in contact line problems (Bonn *et al.* 2009; Snoeijer & Andreotti 2013; Vandre *et al.* 2014; Sprittles 2015) in order to regularise the local flow and to thus allow contact line motion, but is usually not important elsewhere in the flow. The inner length scale λ is contrasted with an outer 'macroscopic' length scale R, for example the radius of a spreading drop or the capillary length scale in the problem.

Cox (1986) clarified the structure of low capillary number problems in terms of the ratio $\epsilon = \epsilon_0\lambda/R$ between the two length scales; ϵ_0 is a numerical factor to be determined. From a general analysis, Cox (1986) obtained

$$g(\theta_{\rm eq}) = g(\theta_{\rm app}) + {\rm Ca}\ln\epsilon, \tag{1.1}$$

where

$$g(\theta) = \int_0^\theta \frac{u - \cos u \sin u}{2\sin u} du \tag{1.2}$$

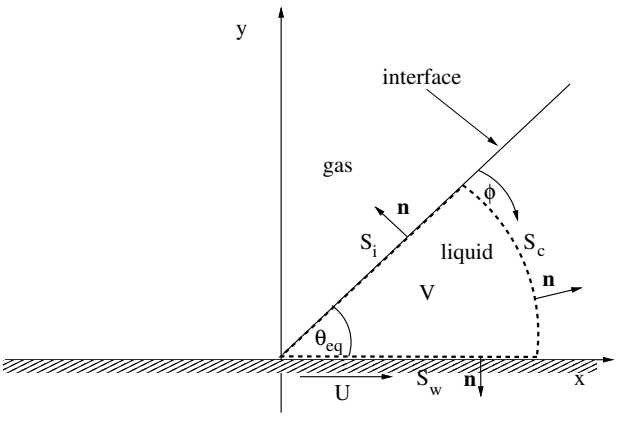

FIGURE 1. Sketch of geometry; the volume of integration is shown as the dotted line.

for a single phase (a liquid volume, neglecting the effect of a surrounding gas). Here, $\theta_{\rm eq}$ is the (equilibrium) contact angle on the microscopic scale, and $\theta_{\rm app}$ is the apparent contact angle of the spreading drop, obtained by fitting a spherical cap to its shape. In Cox's analysis, the dimensionless capillary number

$$\mathrm{Ca} = \frac{U\eta}{\gamma} \tag{1.3}$$

is assumed small, where U is the speed of the contact line. Here, η is the fluid viscosity, and γ is the surface tension. For steady flow, it is often more convenient to instead think of the contact line being stationary and the wall to be moving at speed U, because we can then think of the interface as time-independent.

All that remains is to calculate the factor ϵ_0 which determines the effective value of the ratio of the two length scales. The advantage of (1.1) is that ϵ_0 can be determined from solving two separate *linear* problems (Eggers & Fontelos 2015). Near the contact line, one has to find the deviation of the contact angle from $\theta_{\rm eq}$, on the microscopic (inner) scale λ. On the scale of the drop, the objective is to find the deviation from $\theta_{\rm app}$ as the substrate is approached from the drop (the outer scale). In the present paper, we focus on the matching of the interface slope to a slip surface for arbitrary contact angles, and for two-phase flows with arbitrary viscosities. The other part of the problem, matching to the quasistatic drop surface, has to our knowledge not been done for general angles.

An approach to describe the shape of the interface is to write (1.1) as an evolution equation for the local slope θ, as in Snoeijer (2006) and Chan *et al.* (2013) for a single phase and two-phase systems, respectively. For simplicity, we neglect external forcing (such as by gravity), which only becomes important on a macroscopic scale. The requirement that the interface (described by its thickness $h(s)$), is assumed steady, while the substrate is moving at speed U to the right, then leads to the GL (generalized lubrication) equation. One obtains

$$\frac{d^2\theta}{ds^2} = \frac{3\mathrm{Ca}F(\theta, M)}{h^2}, \tag{1.4}$$

where s is the arclength along the interface, and $M = \eta_g/\eta_l$ the ratio of the viscosity of the outer phase (for example a gas), and the viscosity of the liquid (cf. Fig. 1). In the

case of a single (liquid) phase only,

$$F(\theta) \equiv F(\theta, 0) = -\frac{2\sin^3\theta}{3(\theta - \sin\theta\cos\theta)}. \tag{1.5}$$

Here, $F(\theta)$ is related to $g(\theta)$ by $F(\theta) = (2/3)\sin^2\theta g(\theta)$. The full expression $F(\theta, M)$ for two fluids is given in (2.11). To close (1.4), one has to simultaneously solve the geometrical relations

$$\frac{dh}{ds} = \sin\theta, \quad \frac{dx}{ds} = \cos\theta. \tag{1.6}$$

to find the interface shape $h(x)$ in a Cartesian coordinate system. Integrating (1.4), making use of the limit of small Ca, (1.6) leads precisely to the structure given by (1.1).

To build the crossover to the slip region into the GL equation, we follow Chan *et al.* (2013) and introduce the modified GL equation

$$\frac{d^2\theta}{ds^2} = \frac{3\mathrm{Ca}F(\theta, M)}{h(h + c\lambda)}, \tag{1.7}$$

where c is a constant to be chosen such that the solution matches properly with the slip region. In Chan *et al.* (2013) this was done assuming that $c = 3$, which is true only for small angles and for a single phase (Hocking 1983). Here, we calculate the dependence of c on the microscopic contact angle θ_{eq} and on the viscosity ratio M. Once c is known, one has to integrate (1.7) from the contact line to whichever macroscopic configuration is required for the problem.

Let us start by sketching the structure of the analysis to compute c. It is sufficient to consider a linear perturbation of the free surface shape around a wedge with microscopic (equilibrium) angle θ_{eq}. Therefore we set $\theta = \theta_{\mathrm{eq}} - \varphi(s)$, and, to linear order in φ, all calculations can be performed assuming a wedge geometry $h = s\sin\theta_{\mathrm{eq}}$ for the flow (cf. Fig. 1). Linearizing (1.7) in φ and integrating twice, we have

$$\varphi = \frac{3\mathrm{Ca}F(\theta_{\mathrm{eq}}, M)}{\sin^2\theta_{\mathrm{eq}}}\left[\frac{h}{c\lambda}\left(\ln(h + c\lambda) - \ln h\right) + \ln(h + c\lambda) - 1\right] + Ch + C_1.$$

We are interested in solutions which only grow logarithmically, corresponding to vanishing curvature at infinity, and so $C = 0$. From the boundary condition $\varphi(0) = 0$ it follows that $C_1 = 3\mathrm{Ca}F(\theta_{\mathrm{eq}}, M)(1 - \ln c\lambda)/\sin^2\theta_{\mathrm{eq}}$, and so to leading order as $s/\lambda \to \infty$ we have

$$\varphi(s) = \frac{3\mathrm{Ca}F(\theta_{\mathrm{eq}}, M)}{\sin^2\theta_{\mathrm{eq}}}\ln\frac{se\sin\theta_{\mathrm{eq}}}{c\lambda}. \tag{1.8}$$

Here, we calculate c for arbitrary angles θ_{eq} and arbitrary viscosity ratios M, based on earlier work by Hocking (1977), who calculates the stress on a slip wall, assuming a straight interface $h = s\sin\theta_{\mathrm{eq}}$. Using the fact that in the absence of inertia (Stokes dynamics), the total force on any fluid volume vanishes, we can convert the wall force to a force on the interface, which leads to bending of the interface, allowing us to determine c. In addition, one may also allow for an arbitrary ratio of slip lengths λ_1/λ_2 at the two fluid-solid interfaces, but no explicit results are available for this case. So in the interest of simplicity, we will always assume $\lambda_1 = \lambda_2 \equiv \lambda$.

2. Determining c from a force balance

2.1. *A single phase*

We start the analysis by considering the case of a single phase (the liquid, as shown in Fig. 1), which enables us to show some of the calculations in greater detail. The idea is to consider a force balance over the volume shown in Fig. 1, within which the Stokes equation $\boldsymbol{\nabla}\cdot\boldsymbol{\sigma}=0$ is satisfied; $\boldsymbol{\sigma}$ is the stress tensor. Using Gauss' theorem, and only considering the force in the x-direction, we obtain

$$\int_S \mathbf{n}\cdot\boldsymbol{\sigma}\cdot\mathbf{e}_x = 0, \tag{2.1}$$

where $\mathbf{n}$ is the outward normal, and $S=S_i+S_c+S_w$. The volume is the slice of radius s inside the fluid, where S_i is the fluid-gas interface, S_c a circular arc of radius s inside the fluid, and S_w the wall, see Fig. 1.

The force on V coming from the interface is

$$\int_{S_i}\mathbf{n}\cdot\boldsymbol{\sigma}\cdot\mathbf{e}_x ds = -\gamma\int_{S_1}\kappa\mathbf{n}\cdot\mathbf{e}_x ds \simeq \gamma\sin\theta_{\mathrm{eq}}\int_0^s\frac{d\varphi}{ds}ds = \gamma\sin\theta_{\mathrm{eq}}\varphi(s). \tag{2.2}$$

Here, we have used the stress boundary condition (Landau & Lifshitz 1984) $\mathbf{n}\cdot\boldsymbol{\sigma}=-\gamma\mathbf{n}\kappa$, where $\kappa=d\varphi/ds$ is the interface curvature and $\boldsymbol{n}\cdot\mathbf{e}_x\simeq-\sin\theta_{\mathrm{eq}}$. The integral over S_w, representing the total force w on the wall between the origin and $x=s$, has been calculated by Hocking (1977) for Stokes flow in a corner with slip at the wall, and a free-slip condition at the interface. The contribution v of the force on S_c can be inferred from the far-field limit of the flow, calculated by Huh & Scriven (1971). Thus (2.1) gives

$$\gamma\sin\theta_{\mathrm{eq}}\varphi(s) = -v-w, \tag{2.3}$$

which we compare to (1.8) to find c.

To find v and w, we need to consider the flow in the wedge-shaped fluid domain (cf. Fig. 1) of opening angle $\theta=\theta_{\mathrm{eq}}$. In Hocking (1977), the flow is solved subject to the slip boundary condition (with u the horizontal component of the velocity)

$$u(x,0) = U+\lambda\frac{\partial u}{\partial y}$$

on the wall. It is convenient to count the angle ϕ from the interface; the velocity field is given in terms of the stream function

$$u_r=\frac{1}{r}\frac{\partial\psi}{\partial\phi},\quad u_\phi=-\frac{\partial\psi}{\partial r}.$$

The boundary conditions on both boundaries are zero normal velocity, and vanishing shear stress $\sigma_{r\phi}=0$ on the interface. Thus for $\phi=\theta_{\mathrm{eq}}$ (the wall) we have

$$\frac{\partial\psi}{\partial r}=0,\quad U=\frac{1}{r}\frac{\partial\psi}{\partial\phi}+\frac{\lambda}{r^2}\frac{\partial^2\psi}{\partial\phi^2},$$

and for $\phi=0$ (the interface)

$$\frac{\partial\psi}{\partial r}=0,\quad \frac{1}{r^2}\frac{\partial^2\psi}{\partial\phi^2}-\frac{\partial^2\psi}{\partial r^2}+\frac{1}{r}\frac{\partial\psi}{\partial r}=0.$$

In the limit $r\gg\lambda$ we can neglect the effects of slip, and we should fall back on the similarity solution $\psi=rf(\theta_{\mathrm{eq}})$ found by Huh & Scriven (1971). With the ansatz

$$f=a_1\sin\phi+a_2\cos\phi+a_3\phi\sin\phi+a_4\phi\cos\phi, \tag{2.4}$$

the boundary conditions are

$$f(0) = 0, \quad f''(0) = 0, \quad f(\theta_{\rm eq}) = 0, \quad f'(\theta_{\rm eq}) = U.$$

The coefficients are ($D = \theta_{\rm eq} - \sin\theta_{\rm eq}\cos\theta_{\rm eq}$),

$$a_1 = -\frac{U\theta_{\rm eq}\cos\theta_{\rm eq}}{D}, \quad a_2 = 0, \quad a_3 = 0, \quad a_4 = -\frac{U\sin\theta_{\rm eq}}{D},$$

and so the stresses become

$$\sigma_{rr} = \frac{2\eta U}{rD}\sin\theta_{\rm eq}\cos\phi, \quad \sigma_{r\phi} = \frac{2\eta U}{rD}\sin\theta_{\rm eq}\sin\phi. \tag{2.5}$$

Using (2.5), and

$$\mathbf{n}\cdot\boldsymbol{\sigma}\cdot\mathbf{e}_x = \sigma_{rr}\cos(\theta_{\rm eq}-\phi) + \sigma_{r\phi}\sin(\theta_{\rm eq}-\phi),$$

we find

$$v = \int_{S_c}\mathbf{n}\cdot\boldsymbol{\sigma}\cdot\mathbf{e}_x ds = r\int_0^{\theta_{\rm eq}}\mathbf{n}\cdot\boldsymbol{\sigma}\cdot\mathbf{e}_x d\phi = -\frac{3\eta U F(\theta_{\rm eq})}{\sin\theta_{\rm eq}},$$

where $F(\theta_{\rm eq})$ is the angle dependence from the GL model given previously in (1.5). As an aside, $F(\theta_{\rm eq})$ can easily be calculated from $\sigma_{\phi\phi}$, evaluated at the interface $\phi = 0$, and using the stress boundary condition $\gamma\kappa = -\sigma_{\phi\phi}|_{\phi=0}$. On the other hand, using $h = s\sin\theta_{\rm eq}$ and integrating (1.4) once, we have

$$\kappa = \frac{d\varphi}{ds} = \frac{3{\rm Ca}F(\theta_{\rm eq})}{s\sin^2\theta_{\rm eq}}; \tag{2.6}$$

comparing with $\sigma_{\varphi\varphi}|_{\phi=0}$ yields $F(\theta_{\rm eq})$.

Finally Hocking (1977) has calculated the force on the wall

$$w = \int_{S_w}\mathbf{n}\cdot\boldsymbol{\sigma}\cdot\mathbf{e}_x ds = -\int_{S_w}\sigma_{xy} ds = U\eta\left[-\frac{3F(\theta_{\rm eq})}{\sin\theta_{\rm eq}}\ln\frac{s}{\lambda} + h_1\right],$$

where $h_1(\theta_{\rm eq})$ is known numerically. Known values are $h_1(\pi/2) = 4(\gamma_E - \ln 2)/\pi$, while for small $\theta_{\rm eq}$, $h_1 = -3\ln(3/\theta_{\rm eq})/\theta_{\rm eq}$. Using (2.3), it follows that in the general case

$$\varphi(s) = {\rm Ca}\left[\frac{3F(\theta_{\rm eq})}{\sin^2\theta_{\rm eq}}\ln\frac{se}{\lambda} - \frac{h_1}{\sin\theta_{\rm eq}}\right],$$

which is precisely of the expected form (1.8). Comparing the two, we find

$$c = \sin\theta_{\rm eq}\exp\left(\frac{\sin\theta_{\rm eq}h_1(\theta_{\rm eq})}{3F(\theta_{\rm eq})}\right), \tag{2.7}$$

which is our main result in the case of a single phase.

The result is shown in Fig. 2 for a range of angles. For small $\theta_{\rm eq}$, one recovers $c = 3$ as known from lubrication theory; for $\theta_{\rm eq} = \pi/2$,

$$c(\pi/2) = e^{\ln 2 - \gamma_E} \approx 1.12, \tag{2.8}$$

smaller by about a factor of three. Interestingly, c becomes very small for angles close to π. For example, $c(0.9\pi) = 1.04\cdot 10^{-4}$, showing that in general c cannot be inferred from a comparison with lubrication theory.

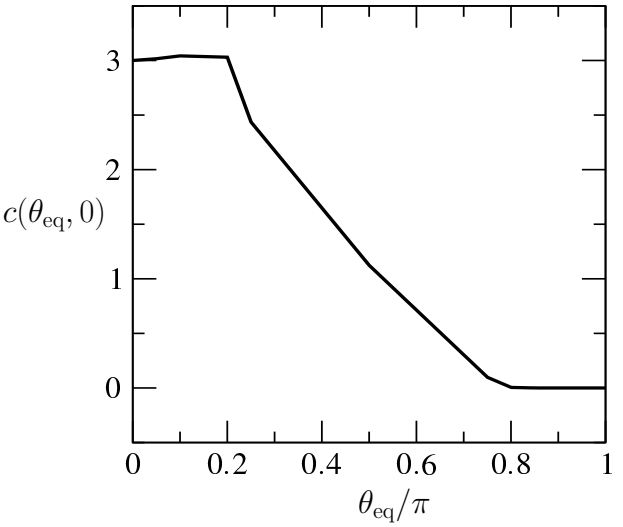

FIGURE 2. The c-factor as function of $\theta_{\rm eq}/\pi$ for $M = 0$, calculated from the tabulated values for h_1 in Hocking (1977).

2.2. *Two phases*

We now generalize to the case of two phases (arbitrary viscosity ratios M), for which the constant c has never been calculated, not even for small angles. We explain the general structure, but explicit results are available for $\theta_{\rm eq} = \pi/2$ only.

In contrast to the previous subsection, we now have the integral (2.1) over the surface of two volumes V_1 and V_2; V_1 is the volume over the "liquid" phase as before (labeled 1), V_2 is the corresponding slice of the same radius s over phase 2 (the "gas"). Then (2.1), written for each phase, becomes

$$\int_{S_i} \mathbf{n} \cdot \boldsymbol{\sigma}_1 \cdot \mathbf{e}_x + v_1 + w_1 = 0, \quad -\int_{S_i} \mathbf{n} \cdot \boldsymbol{\sigma}_2 \cdot \mathbf{e}_x + v_2 + w_2 = 0, \tag{2.9}$$

where v and w have the same meanings as before, but for each phase separately. Using the stress condition $\mathbf{n} \cdot (\boldsymbol{\sigma}_1 - \boldsymbol{\sigma}_2) = -\gamma \mathbf{n} \kappa$, this yields

$$\gamma \sin\theta_{\rm eq} \varphi(s) = -v_1 - v_2 - w_1 - w_2. \tag{2.10}$$

The solution for a no-slip flow, for general M, has been given by Huh & Scriven (1971). At the interface between the two fluids we now have continuity of the tangential velocity (the normal velocity vanishes), and of shear stress. If the stream functions in either phase are $\psi_{1/2} = r f_{1/2}(\theta_{\rm eq})$, the boundary conditions are

$$f_1(0) = f_2(0) = 0, \quad f_1''(0) = M f_2''(0), \quad f_1'(0) = f_2'(0), \quad f_1(\theta_{\rm eq}) = 0,$$
$$f_1'(\theta_{\rm eq}) = U, \quad f_2(\theta_{\rm eq} - \pi) = 0, \quad f_2'(\theta_{\rm eq} - \pi) = -U.$$

The results are a little too complicated to write out here, but as in (2.6), we can calculate the general form of $F(\theta, M)$ in (1.4), by computing the normal stress on the interface from either phase, giving

$$\sigma^{(2)}_{\phi\phi}\Big|_{\phi=0} - \sigma^{(1)}_{\phi\phi}\Big|_{\phi=0} = \gamma\kappa = \frac{3U\eta}{r \sin^2\theta_{\rm eq}} F(\theta_{\rm eq}, M).$$

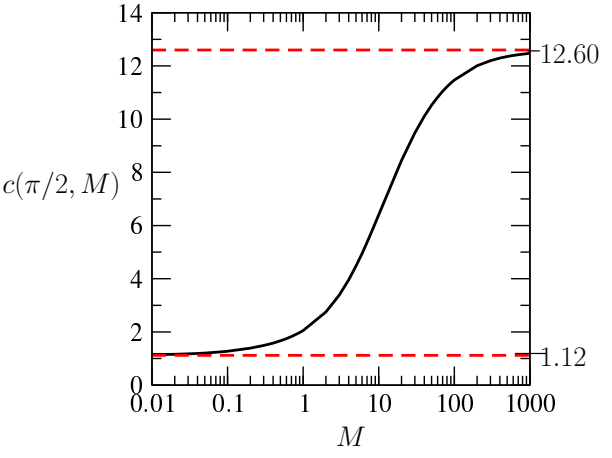

FIGURE 3. The c-factor as function of $\log_{10} M$ for $\theta_{\rm eq} = \pi/2$. Horizontal (red) dashed lines are the asymptotes of c for $M = 0$ ($c \approx 1.12$) and $M \to \infty$ ($c \approx 12.60$).

Comparison with (1.4) then shows that

$$F(\theta, M) = -\frac{2\sin^3\theta}{3}\frac{M^2 F_1(\theta) + 2MF_3(\theta) + F_1(\pi-\theta)}{MF_1(\theta)F_2(\pi-\theta) + F_1(\pi-\theta)F_2(\theta)}, \tag{2.11}$$

where

$$F_1 = \theta^2 - \sin^2\theta, \quad F_2 = \theta - \sin\theta\cos\theta, \quad F_3 = \theta(\pi-\theta) + \sin^2\theta;$$

note the sign error in Chan *et al.* (2013).

Furthermore, it follows from the Huh-Scriven solution, after a lengthy but elementary calculation, that

$$v_1 + v_2 = -\frac{3U\eta F(\theta_{\rm eq}, M)}{\sin\theta_{\rm eq}}.$$

The shear force on the wall now has contributions from both phases, and it follows from Hocking (1977) that

$$w_1 + w_2 = U\eta\left[-\frac{F(\theta_{\rm eq}, M)}{\sin\theta_{\rm eq}}\ln\frac{s}{\lambda} + h_1 + Mh_2\right].$$

Taken together with (2.10), this yields the interface deformation

$$\varphi(s) = {\rm Ca}\left[\frac{3F(\theta_{\rm eq}, M)}{\sin^2\theta_{\rm eq}}\ln\frac{se}{\lambda} - \frac{h_1 + Mh_2}{\sin\theta_{\rm eq}}\right],$$

and comparing with (1.8)

$$c = \sin\theta_{\rm eq}\exp\left(\frac{\sin\theta_{\rm eq}(h_1 + Mh_2)}{3F(\theta_{\rm eq}, M)}\right), \tag{2.12}$$

now involving two numerical constants h_1 and h_2. This completes our calculation, but it remains to calculate the constants h_1 and h_2, which are functions of $\theta_{\rm eq}$ and M. According to Hocking (1977) this can be done explicitly for a right angle $\theta_{\rm eq} = \pi/2$, for which

$$h_1 = \frac{(1-M)h_a + 2Mh_b}{1+M}, \quad h_2 = \frac{-(1-M)h_a + 2Mh_b}{1+M}, \tag{2.13}$$

where $h_a = (4/\pi)(\gamma_E - \ln 2)$ and $h_b = -1.539$. The geometrical factor is

$$F(\pi/2, M) = -\frac{4}{3\pi}\frac{(M+1)^2\pi^2 - 4(M-1)^2}{(\pi^2-4)(M+1)} \tag{2.14}$$

for right angles. It is now a simple matter to compute the c-factor, shown in Fig. 3, as a function of $\log_{10} M$. For small M (to the left of the figure), one recovers (2.8). For large M, on the other hand, c rises significantly towards $c \to \exp(-\pi(h_a + 2h_b)/4) \approx 12.60$ as $M \to \infty$, showing once more that the behavior for finite angles is significantly different from the lubrication result.

3. Discussion

To illustrate and validate our results, we consider a plate being pushed into a container of liquid 2, with an outer liquid 1, as shown in Fig. 4 (a). We compare full numerical simulations of this problem, using the finite elements method (FEM) described in detail in Kamal *et al.* (2018), and based on a framework benchmarked in (Sprittles 2015), with results of the GL equation for Ca up to 0.1. We show an example with $M = 0$ and one with $M = 1$, with a contact angle of $\pi/2$ (Fig. 4 (b) and (c), respectively). On the left, the solid line is the interface profile found from FEM, the red dashed line comes from integrating (1.7) using the expression of c in (2.7), as obtained by the present theory; very good agreement is found.

To demonstrate the importance of using the correct value of c in order to obtain this agreement, we also plot the profile obtained using the value $c = 3$, proposed previously (Snoeijer 2006; Chan *et al.* 2013). However, this value is only appropriate in the limit of small contact angles and no outer fluid ($M = 0$). As a result, the dot-dashed blue, which is the profile thus obtained from the GL equation, differs significantly from the "exact" result, obtained from direct numerical simulation.

In order to focus on the solution very close to the contact line, we also plot the relative deviation between the FEM simulation and solutions obtained from integrating (1.7) on the right of Fig. 4. For the solid line we use the correct value of c, the dashed line represents the value $c = 3$. For the smaller capillary number, using the c-value as calculated in the present paper, the deviation is negligible, and even for a capillary number $\mathrm{Ca} = 0.1$, the relative error remains small; when the capillary number becomes of order unity the GL equation fails (Kamal *et al.* 2018), since it is an expansion for small Ca only. On the other hand for $c = 3$ the relative error is significant in both cases, as one approaches the contact line.

In conclusion, we have analyzed the Cox-Voinov theory with slip, for arbitrary contact angles and arbitrary viscosity ratios. Closed form expressions are provided using the generalized lubrication equation, which is shown to be a powerful tool to calculate interface flows involving moving contact lines in situations in which the interface slope is not necessarily small. The present paper provides a consistent version of the GL equation for arbitrary contact angles.

Acknowledgments

This work has been financially supported by EPSRC (UK) grants (EP/N016602/1, EP/P020887/1 & EP/P031684/1). T. S. C. gratefully acknowledges financial support from the UiO: Life Science initiative at the University of Oslo. J. E. acknowledges the support of Leverhulme Trust International Academic Fellowship IAF-2017-010.

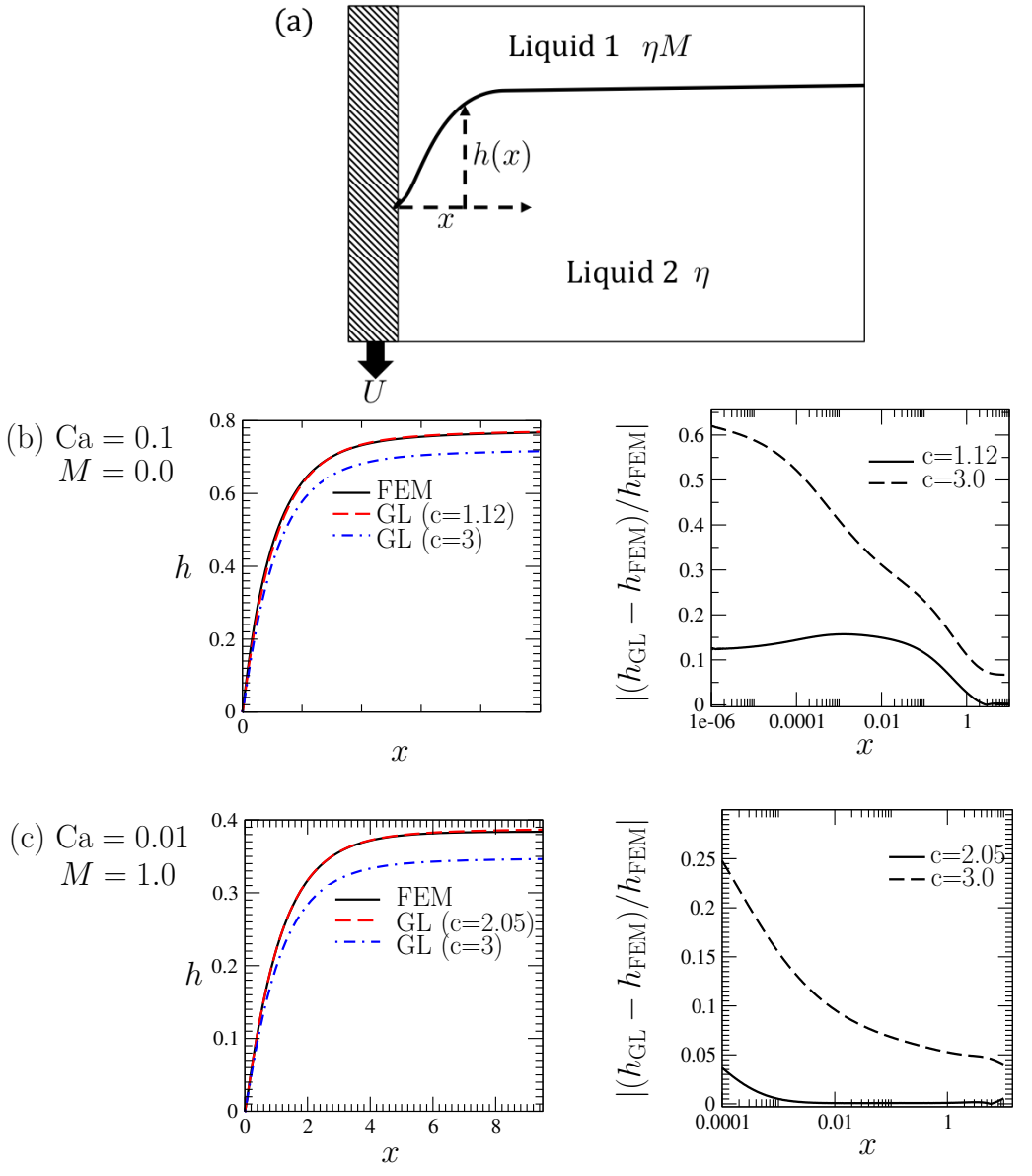

FIGURE 4. (a): Sketch of the interface shape between two liquids produced by a descending plate; all lenghts are in units of λ. (b) & (c): Comparison of interface profiles from FEM with GL simulations for i) the correct value of $c(\pi/2, M)$ and ii) the previously used value $c(0, M = 0) = 3$ for Ca $= 0.1$, $M = 0$ and Ca $= 0.01$, $M = 1$, respectively. Left: Steady profiles, right: relative error of the GL profile h_{GL} compared to FEM profile h_{FEM}.

REFERENCES

BARRAT, J.-L. & BOCQUET, L. 1999 Large slip effect at a nonwetting fluid-solid interface. *Phys. Rev. Lett.* **82**, 4671–4674.

BONN, D., EGGERS, J., INDEKEU, J., MEUNIER, J. & ROLLEY, E. 2009 Wetting and spreading. *Rev. Mod. Phys.* **81**, 739–805.

CHAN, T. S., SRIVASTAVA, S., MARCHAND, A., ANDREOTTI, B., BIFERALE, L., TOSCHI, F. &

Snoeijer, J. H. 2013 Hydrodynamics of air entrainment by moving contact lines. *Phys. Fluids* **25**, 074105.

Cottin-Bizonne, C., Cross, B., Steinberger, A. & Charlaix, E. 2005 Boundary slip on smooth hydrophobic surfaces: intrinsic effets and possible artifacts. *Phys. Rev. Lett.* **94**, 056102.

Cox, R. G. 1986 The dynamics of the spreading of liquids on a solid surface. Part 1. Viscous flow. *J. Fluid Mech.* **168**, 169–194.

Eggers, J. & Fontelos, M. A. 2015 *Singularities: Formation, Structure, and Propagation*. Cambridge University Press, Cambridge.

Hocking, L. M. 1977 A moving fluid interface. Part 2. The removal of the force singularity by a slip flow. *J. Fluid Mech.* **79**, 209–229.

Hocking, L. M. 1983 The spreading of a thin drop by gravity and capillarity. *Q. J. Mech. Appl. Math.* **36**, 55–69.

Huh, C. & Scriven, L. E. 1971 Hydrodynamic model of steady movement of a solid/liquid/fluid contact line. *J. Coll. Int. Sci.* **35**, 85–101.

Kamal, C., Sprittles, J., Snoeijer, J. H. & Eggers, J. 2018 Dynamic drying transition via free-surface cusps. *J. Fluid Mech.* **858**, 760.

Landau, L. D. & Lifshitz, E. M. 1984 *Fluid Mechanics*. Pergamon: Oxford.

Lauga, E., Brenner, M. P. & Stone, H. A. 2008 Microfluidics: the no-slip boundary condition. In *Springer Handbook of Experimental Fluid Mechnaics* (ed. C. Tropea, J. F. Foss & A. Yarin), pp. 1219–1240. Springer.

Snoeijer, J. H. 2006 Free surface flows with large slopes: beyond lubrication theory. *Phys. Fluids* **18**, 021701.

Snoeijer, J. H. & Andreotti, B. 2013 Moving contact lines: scales, regimes, and dynamical transitions. *Annu. Rev. Fluid Mech.* **45**, 269–292.

Sprittles, J. E. 2015 Air entrainment in dynamic wetting: Knudsen effects and the influence of ambient air pressure. *J. Fluid Mech.* **769**, 444–481.

Vandre, E., Carvalho, M. S. & S, Kumar 2014 Characteristics of air entrainment during dynamic wetting failure along a planar substrate. *J. Fluid Mech.* **747**, 119–140.

Voinov, O. V. 1976 Hydrodynamics of wetting [english translation]. *Fluid Dynamics* **11**, 714–721.